

X-ray Structural Studies and Physicochemical Characterization of the 1-Butanol, 1-Pentanol, and 1,4-Dioxane Solvates of Succinylsulfathiazole

SUSAN A. BOURNE, MINO R. CAIRA^x, LUIGI R. NASSIMBENI, AND INNOCENT SHABALALA

Received September 7, 1993, from the *Department of Chemistry, University of Cape Town, Rondebosch 7700, Cape Province, South Africa.* Accepted for publication December 13, 1993^o.

Abstract □ The crystal structures and thermal decomposition of three solvated forms of the antibacterial drug succinylsulfathiazole (SST) have been studied. The solvates, with 1:1 host-guest stoichiometry, are SST·1-butanol (1) SST·1-pentanol (2), and SST·1,4-dioxane (3). Solvates 1 and 2 crystallize in the triclinic system, space group *P*1, with two formula units per cell, and are nearly isostructural. The OH groups of the guest molecules in both solvates engage in hydrogen bonding to the host SST and occupy cavities in the crystals. Solvate 3 is triclinic, space group *P*1, with two formula units per cell, but the two independent solvent molecules are located in crystallographically distinct channels. In one channel, solvent molecules are hydrogen bonded to the host while, in the other, they are held by van der Waals interactions only. The structural results are in accord with thermogravimetric and differential scanning calorimetric data which indicate one-step desolvation for 1 and 2 but two-step desolvation for 3. X-ray powder diffraction was used to attempt identification of the polymorphic forms of SST resulting from desolvation of 1–3. Desolvation of 1 and 3 appears to yield pure polymorphs of SST while 2 yields a mixture of polymorphs. The activation energies for the desolvation of the nearly isomorphous solvates 1 and 2 were found by dynamic thermogravimetry to be 155 and 149 kJ mol⁻¹, respectively.

Succinylsulfathiazole [4'-(2-thiazolylsulfamoyl)succinamic acid], hereinafter SST (see chemical structure shown in Figure 1), is an antibacterial drug which is poorly absorbed. Its long duration of action is attributed to the slow liberation of sulfathiazole in the bowel by hydrolytic removal of the succinyl residue.¹ In a recent study of this drug,² six anhydrous crystal forms, three polymorphic monohydrates as well as an acetone and an 1-butanol solvate were identified. Crystalline solvated drug species are of interest because entrapment of the solvent molecules in cavities formed by the host drug lattice can yield very stable clathrates, as we observed recently for solvates of 5-methoxysulfadiazine.³ Desolvation of such species can result in effective particle size reduction in the preparation of pure polymorphic forms of the parent drug, as has been illustrated for solvates of sulfathiazole.⁴

The 1-butanol solvate (1) of SST was reported to contain 0.86 mol of solvent/mol of drug² while in an earlier study⁵ a 1-pentanol solvate (2) of this drug, with 0.9 mol of solvent/mol of drug, was reported. The latter solvate has been cited as showing a remarkable increase in bioavailability relative to the unsolvated drug.⁶ Only one crystallographic analysis of a solvate of SST, that of a monohydrate, has appeared in the literature.⁷ The lack of structural information regarding the nature of solvent inclusion by succinylsulfathiazole as well as the unusual stoichiometric proportions reported for the solvates prompted us to prepare 1 and 2 and determine their crystal structures by X-ray methods. We have also prepared a new species, namely a 1,4-dioxane solvate (3) of the drug. We have investigated the thermal decomposition of 1–3 by thermal analysis and X-ray powder diffraction. This paper reports the X-ray crystallographic structure determination of succinylsulfathiazole sol-

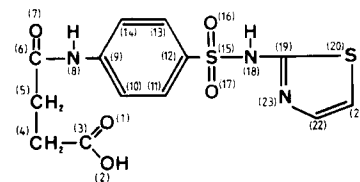


Figure 1—Chemical structure of succinylsulfathiazole and atomic numbering used in this study.

vates 1–3 and the thermodynamics and kinetics of their desolvation in relation to their crystal structures.

Experimental Section

Materials—The raw material and the product obtained by dehydrating it were characterized by thermal analysis and X-ray powder diffraction. Anhydrous succinylsulfathiazole was obtained by dehydrating the commercially available monohydrate (Sigma Chemical Co., St. Louis, MO) at 105 °C for 17 h. Further vacuum-drying for 5 h ensured complete dehydration as indicated by differential scanning calorimetry (DSC) and thermogravimetric (TG) measurements. The solvents 1-butanol, 1-pentanol, and 1,4-dioxane were predried over molecular sieves for several days.

Crystal Preparation—The solvates were prepared by dissolving 200 mg of the anhydrous drug in 40 mL of each solvent with vigorous stirring and heating to just below their boiling points. Well-developed prismatic crystals formed within 24 h on slow cooling of the hot solutions.

X-ray Powder Diffractometry—X-ray powder patterns were recorded with a Philips PW1050/80 vertical goniometer using Ni-filtered Cu K α radiation ($\lambda = 1.5418$ Å).

Instrumental settings were as follows: 40 kV, 30 mA, divergence and receiving slits 1° each, angular range 2θ 6–40°; scan speed 1° 2θ min⁻¹. Surface solvent was removed from the solvate crystals which were then lightly ground in an agate mortar and packed in aluminum sample holders.

Calculated X-ray Patterns—The program Lazy Pulverix⁸ was used to generate several simulated X-ray powder patterns. The input data, obtained from the literature or from the single-crystal structure analyses reported here, consisted of unit cell data, space group symmetry, atomic positions, and thermal parameters. Patterns were calculated over the angular range 2θ 6–40° for Cu K α radiation ($\lambda = 1.5418$ Å).

Thermal Analysis—TG and DSC analyses of the solvates were carried out using, respectively, a Perkin-Elmer TGA 7 balance and a Perkin-Elmer DSC 7 instrument calibrated with indium and zinc standards. For TG, 5–10-mg samples were heated at 10 °C min⁻¹ from 30–250 °C under a constant N₂ purge. The same heating rate and temperature range were employed for the DSC measurements with the samples sealed in vented pans. For the kinetic studies, TG traces were obtained at several heating rates in the range 1–50 °C min⁻¹.

X-ray Structure Analyses—Clear, colorless single crystals of the solvates became opaque within 2 h due to desolvation under atmospheric conditions. For preliminary X-ray photography and for intensity data collections at 294 K, all specimens were mounted in their mother liquor in sealed Lindemann capillaries. Weissenberg and precession photographs indicated Laue symmetry $\bar{1}$ (triclinic system) for 1–3.

Intensities in the θ range 1–25° were measured on an Enraf-Nonius CAD4-diffractometer using Mo K α radiation ($\lambda = 0.7107$ Å). In each case, accurate cell parameters were obtained by least-squares refinement of the setting angles of 24 reflections ($32^\circ \leq 2\theta \leq 34^\circ$) and intensity data were collected using the ω - 2θ scan mode with variable scan speeds and a maximum recording time of 40 (1 and 3) and 60 s (2) per reflection.

^o Abstract published in *Advance ACS Abstracts*, February 15, 1994.

Table 1—Crystal Data and Details of Final Refinements

Parameter	1	2	3
Chemical formula	C ₁₃ H ₁₃ O ₅ N ₃ S ₂ ·C ₄ H ₁₀ O	C ₁₃ H ₁₃ O ₅ N ₃ S ₂ ·C ₅ H ₁₂ O	C ₁₃ H ₁₃ O ₅ N ₃ S ₂ ·C ₄ H ₈ O ₂
Formula weight	429.50	443.53	443.49
Space group	P1	P1	P1
a/Å	8.642(2)	8.665(2)	5.647(1)
b/Å	8.931(3)	9.008(1)	12.771(4)
c/Å	14.026(4)	14.198(2)	14.115(6)
α/deg	82.33(3)	82.72(1)	94.48(3)
β/deg	78.40(3)	78.68(1)	100.92(3)
γ/deg	89.40(3)	88.30(2)	99.96(2)
V/Å ³	1050.8(5)	1077.9(3)	978.0(6)
Z	2	2	2
d _{cal} /g cm ⁻³	1.358	1.367	1.506
F(000)	452	468	464
μ(Mo Kα)/cm ⁻¹	2.78	2.73	3.04
Crystal size/mm	0.65 × 0.65 × 0.75	0.50 × 0.50 × 0.25	0.20 × 0.35 × 0.40
Range of indices	0, 10; ±10; ±16	0, 10; ±10; ±16	±6; ±15; 0, 16
Intensities measured	3966	4055	3606
Observed reflections	2965	2338	2393
Observed criterion	I > 3σ(I)	I > 3σ(I)	I > 2σ(I)
R	0.078	0.104	0.054
R _w	0.088	0.107	0.053
Parameters	242	244	271
Max. shift/esd	0.80	0.03	0.01
Δρ excursions/e Å ⁻³	0.67; -0.34	0.83; -0.55	0.53; -0.51

Scan widths varied as $(0.85 + 0.35 \tan \theta)^\circ$ and the aperture width as $(1.12 + 1.05 \tan \theta)$ mm. Three standard reflections were monitored every hour for intensity decay. Orientation control was performed every 200 measured reflections. All data were corrected for Lorentz-polarization effects. Empirical absorption correction factors in the range 0.792–1.000 (1), 0.963–1.000 (2), and 0.976–1.000 (3) were applied. Overall intensity decay values for 1, 2, and 3 were 12.5, 0.5, and 18.9%, respectively. The data for 1 and 3 were corrected for this effect. All corrections were performed using routines of the Enraf-Nonius Structure Determination Package.⁹ Crystal data and details of the refinements are listed in Table 1. Intensity statistics indicated space group P1 as the correct one for 1–3. Structure solution for 2 and 3 involved location of the two independent sulfur atoms per molecule from Patterson syntheses followed by standard Fourier techniques. The close similarity between the cell dimensions of 1 and 2 and their common space group indicated near isomorphism. The non-hydrogen atom positions of the drug molecule in 2 were accordingly used as a phasing model for 1. Solvent molecules were located in difference Fourier ($\Delta\rho$) syntheses.

The 1:1 stoichiometries indicated by TG analysis (see below) for all three solvates were accounted for in the structural models. For 1 and 2 discrete peaks corresponding to the solvent atoms were located in $\Delta\rho$ maps, but their refinement yielded less than satisfactory molecular parameters and abnormally high thermal parameters, as noted previously with, for examples, solvates of 1-butanol.¹⁰ Distance constraints (C–C, 1.54 Å; C–C, 2.515 Å; $\sigma = 0.002$ Å) were thus imposed on the C atoms of the solvent molecules. In the final models, all non-hydrogen atoms except the solvent C atoms were treated anisotropically. The two 1,4-dioxane molecules in the unit cell of 3 were found on different sites of symmetry $\bar{1}$, one of them refining with normal U_{iso} values (0.054–0.063 Å²) and the other with somewhat higher values (0.11–0.13 Å²). In the latter case, a C–C distance constraint of 1.510 Å ($\sigma = 0.002$ Å) was imposed to yield a geometry matching that of the “normal” solvent molecule. All non-hydrogen atoms in 3 were treated anisotropically in the final refinement. Hydrogen atoms for 1–3 were located in $\Delta\rho$ maps and were added in idealized positions at 1.00 Å from their parent atoms. Those of the solvent molecules in 1 and 2 were included at fixed positions with constant $U_{iso} = 0.20$ Å² while all other H atoms were added in a riding model and were assigned common variable U_{iso} values for different chemical groups (e.g. methylene, phenyl) which refined in the range 0.06–0.23 Å². Throughout refinement using the program SHELX76,¹¹ the quantity minimized was $\sum w(|F_o| - |kF_c|)^2$, with w of the form $[\sigma^2(F_o) + gF_o^2]^{-1}$. To ensure the constancy of $\sum (w\Delta F)^2$ with $\sin \theta$, g was assigned the value 0.0 for 2 and 3 and refined to 2.54×10^{-4} for 1.

The precision of the analysis of 2 was somewhat lower than that of 1, as indicated by the esd's of the final parameters and the higher R -factor

for 2. This is attributed to the lower percentage of observed reflections for 2 as well as the need to apply additional constraints, to the geometry of the longer alkyl chain of the solvent 1-pentanol molecule during refinement.

Atomic scattering factors were those cited in the *International Tables for X-ray Crystallography*.¹² Other programs used were PARST¹³ and PLUTO.¹⁴

Information obtained by X-ray structural analysis including final atomic coordinates, bond lengths and angles, torsion angles, mean plane calculations, and structure factor tables, are available from the authors.

Results and Discussion

The atomic numbering scheme of the succinylsulfathiazole molecule in solvates 1–3 is depicted in Figure 1. In view of the variety of the polymorphs (mod. I-mod. VI) and monohydrates (h₁–h₃) reported for SST,² it was necessary to characterize the starting materials and the solvates formed, as well as the species obtained from thermal decomposition of the solvates.

The X-ray powder pattern of the raw material matched that of hydrate h₁ reported by Burger and Grieser.² This powder pattern was also superimposable on that which we calculated using the single crystal X-ray data for a monohydrate of SST published by Rodier et al.⁷ The starting material was thus identified unambiguously. Dehydration of this species yielded a solid whose powder pattern was identical to that published for SST polymorphic form mod. III, of Burger and Grieser.² This was therefore the modification which upon solvation yielded the compounds 1–3 reported here. Experimental X-ray powder patterns for the latter were not always highly reproducible due to varying degrees of decomposition. Following the recommendations of Bar and Bernstein,¹⁵ who maintain that the powder pattern computed from the single crystal structure analysis represents the best model for the pure material, we have used our single-crystal X-ray data for 1–3 to obtain the representative patterns shown in Figure 2. The near isomorphism of 1 and 2 results in very similar patterns for these solvates while the pattern for 3 is distinctly different, as expected from the unit cell data in Table 1. Combined TG and DSC traces for the solvates are shown in Figure 3 and the derived data are listed in Table 2. The

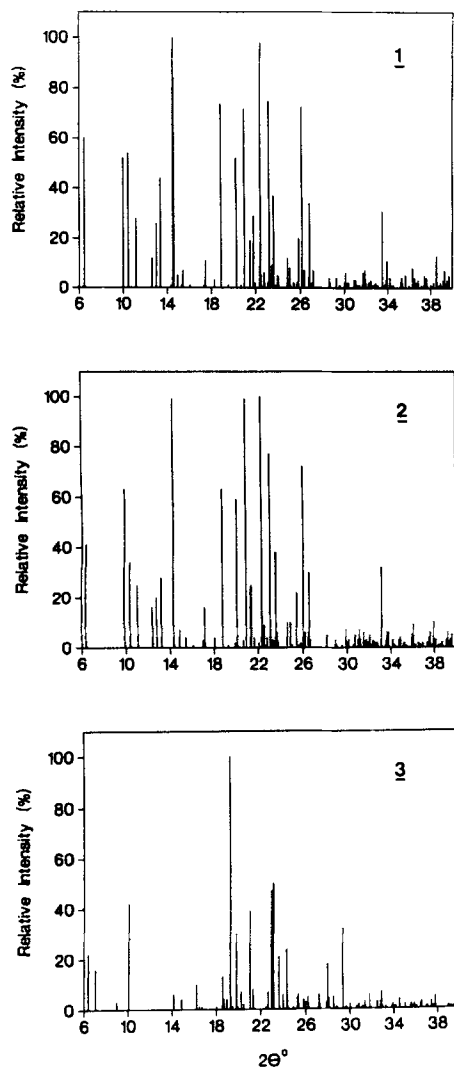


Figure 2—Simulated X-ray powder patterns for the solvates of SST.

TG traces for 1 and 2 indicate that desolvation occurs in one step and the percentage weight losses are consistent with 1:1 host-guest stoichiometries. Desolvation of the 1,4-dioxane solvate 3 proceeds in two distinct steps (Figure 3), the overall percentage weight loss corresponding to a 1:1 ratio for SST:solvent. The individual steps yield 10.9 and 9.1% weight loss, respectively, indicating successive losses of approximately 0.5 mol solvent/mol of SST (theoretical values 9.9 and 9.9%). Prior to the X-ray structure determination of 3, it was inferred from this that the crystals contain 1,4-dioxane molecules in two crystallographically distinct sites with approximately equal frequency. The DSC traces for 1–3 all exhibit three endotherms, with peak A representing complete desolvation in the case of 1 and 2 and partial desolvation for 3. Interpretation of peaks B and C was facilitated by heating each solvate at a temperature approximately 20 °C higher than that of peak A for several hours, followed by recording the X-ray powder pattern of the resulting solid. For 1, the pattern thus obtained corresponded closely to that published for mod. IV of SST.² A double endotherm (peaks B and C, Figure 3) associated with no weight loss in the TG trace also occurs in the published DSC trace of mod. IV (reported onset for peak B, 189 °C). Thus, starting with the raw material, the complete reaction sequence involving solvate 1 was monohydrate $h_1 \rightarrow \text{mod. III} \rightarrow 1 \rightarrow \text{mod. IV}$.

The powder pattern of 2 after desolvation differs from any of those published for the individual polymorphs of SST.² Counterparts for many of the observed peaks were found mainly in

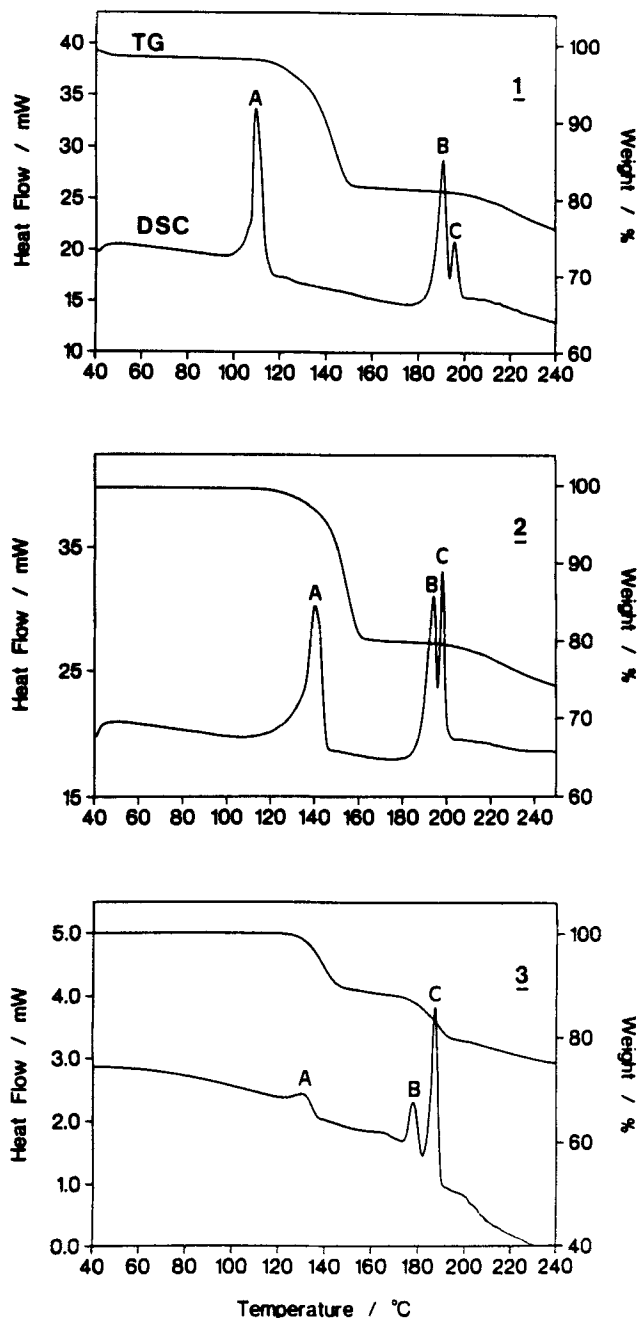


Figure 3—TG and DSC curves for the solvates of SST.

Table 2—TG Weight Losses (%) and DSC Peak Onset Temperatures (°C)

Solvate	Wt Loss 1:1 SST:solvent		Peak Onset °C		
	Calcd	Obsd	A	B	C
1	17.3	17.0	108	187	194
2	19.9	19.7	135	190	197
3	19.9	20.0	123	175	185

the patterns for mod. II–IV, indicating that desolvation of 2 probably yields a mixture of these species. The fusion endotherms B and C in the DSC trace for 2 (Figure 3) occur at temperatures close to those reported for the fusion of mods. II, III, and IV, namely 195, 188–191, and 189–193 °C.

Overlap of melting ranges as well as the reported difficulty of obtaining reproducible melting points for SST polymorphs²

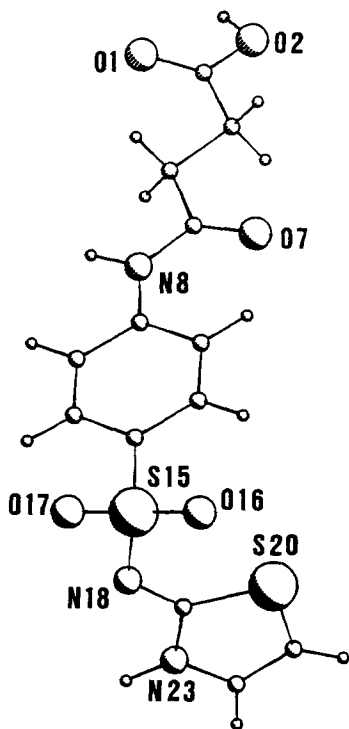


Figure 4—Conformation of the SST molecule in solvate 1.

makes unambiguous assignment of the species present difficult. It is of interest to note that the DSC onset temperatures for release of 1-butanol from 1 and 1-pentanol from 2 (Table 2) are fairly close to the respective normal boiling points of these solvents, namely 118 and 138 °C. The difference between the onset temperature for desolvation and the boiling point of the pure solvent, $T_{on}-T_b$, may be taken as a measure of the thermal stability of a clathrate.¹⁶ On this basis, 1 and 2 are not particularly stable.

When 3 was heated for several hours at 150 °C, the powder pattern of the resulting material resembled that of the original solvate very closely, suggesting that, after loss of approximately 0.5 mol of 1,4-dioxane/mol of SST, the crystal structure is not significantly altered. Endotherm B for 3 (Figure 3), associated with the second stage of solvent release, has its onset at 50 °C higher than that of peak A, indicating significantly tighter binding of the remaining included 1,4-dioxane. This onset temperature also exceeds the normal boiling point of the solvent (101 °C) by 74 °C. The conclusions drawn from the TG and DSC analyses regarding the nature of solvent inclusion in 3 were confirmed by the crystal-structure analysis described below. Peak C (Figure 3) represents fusion of SST. Due to the close proximity of peaks B and C, it was not possible to obtain a powder pattern of fully desolvated 3. From the fusion onset temperature and the appearance of only one fusion peak, the final product of desolvation of 3 appears to be mod. III of SST (reported melting range 188–191 °C).²

Figure 4 shows the conformation adopted by the SST molecule in solvate 1. The principal torsion angles describing this conformation are listed in Table 3 together with the values for corresponding parameters in 2 and 3. The essential features, including the extended side chain which terminates in the carboxylic group and the “syn” arrangement of the two S atoms, are maintained in all three solvates. In all cases, the SST molecule was found to exist in the imido form, with N(23) (rather than N(18), Figure 1) bearing the hydrogen atom. A strong tendency for a specific association between the host SST molecules is indicated by the fact that, in all three solvate crystal structures as well as in monohydrate h_1 ,⁷ the repeating motif of SST is a

Table 3—Torsion Angles (deg) Defining the Conformation Adopted by the SST Molecule in the Solvates

Torsion Angle	1	2	3
O(1)–C(3)–C(4)–C(5)	17.3(8)	11(2)	–3.8(7)
C(3)–C(4)–C(5)–C(6)	–178.2(4)	–179(1)	–178.0(4)
C(4)–C(5)–C(6)–N(8)	–176.7(4)	–177(1)	173.3(4)
C(5)–C(6)–N(8)–C(9)	179.5(5)	180(1)	173.1(4)
C(6)–N(8)–C(9)–C(10)	–176.9(5)	–173(1)	–165.8(5)
C(11)–C(12)–S(15)–N(18)	73.2(5)	73(1)	55.3(4)
C(12)–S(15)–N(18)–C(19)	79.9(4)	80(1)	74.0(4)
S(15)–N(18)–C(19)–S(20)	7.1(7)	4(2)	9.5(6)

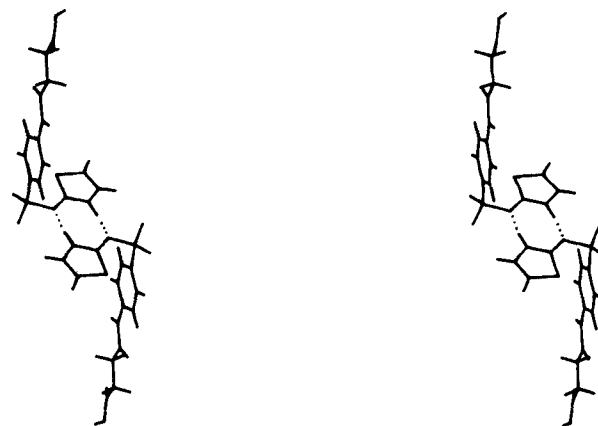


Figure 5—Stereoview of the centrosymmetric hydrogen-bonded dimer of SST which occurs in the solvates.

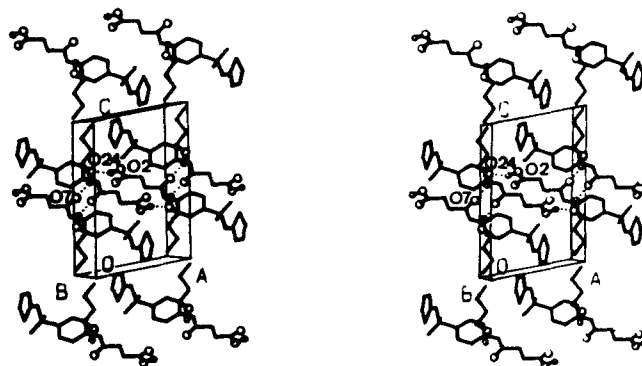


Figure 6—Stereoview of the packing in the unit cell of 1. All H atoms are omitted except those involved in host–guest hydrogen bonding. Hydrogen bonds are indicated by dotted lines.

centrosymmetric dimer containing two identical N(23)–H(23)···N(18) hydrogen bonds. This is shown as a stereoview in Figure 5 for the SST molecules in 1. Since solvates 1 and 2 are nearly isomorphous, the packing diagram for the former only is given in Figure 6 to illustrate the mode of solvent inclusion. The 1-butanol and 1-pentanol molecules in 1 and 2, respectively, are trapped in cavities and engage in analogous hydrogen bonds with the drug molecules. These solvates may therefore be described as “coordination clathrates”.¹⁷ The hydroxyl group of the solvent is both a hydrogen-bond donor and acceptor. Atom O(24) of the solvent molecule accepts a hydrogen bond, O(2)–H(2)···O(24), from the carboxylic group of one SST molecule and donates its H atom in a hydrogen bond, O(24)–H(24)···O(7'), to a carbonyl O atom of a second SST molecule related to the first by unit translation along x . All hydrogen-bond data are listed in Table 4. In solvate 3, all of the 1,4-dioxane molecules are located in channels parallel to [100] as shown in Figure 7, but half of them (at symmetry centers 1/2,0,0) are hydrogen

Table 4—Distances (Å) and Angles (deg) for Hydrogen Bonds

Donor-H		Donor-Acceptor		H...Acceptor		Donor-H...Acceptor Angle	
Solvate 1							
O(2)-H(2)	1.00(2)	O(2)...O(24) ^a	2.624(6)	H(2)...O(24) ^a	1.69(2)	O(2)-H(2)...O(24) ^a	153(3)
O(24)-H(24)	1.00(4)	O(24)...O(7) ^b	2.830(7)	H(24)-O(7) ^b	2.00(7)	O(24)-H(24)...O(7) ^b	138(3)
N(8)-H(8)	1.00(1)	N(8)...O(16) ^c	3.103(6)	H(8)...O(16) ^c	2.12(1)	N(8)-H(8)...O(16) ^c	166(1)
N(23)-H(23)	1.00(1)	N(23)...N(18) ^d	2.825(5)	H(23)...N(18) ^d	1.84(1)	N(23)-H(23)...N(18) ^d	167(1)
Solvate 2							
O(2)-H(2)	1.00(1)	O(2)...O(24) ^a	2.68(2)	H(2)...O(24) ^a	1.69(1)	O(2)-H(2)...O(24) ^a	169(1)
O(24)-H(24)	1.0(1)	O(24)...O(7) ^b	2.83(2)	H(24)-O(7) ^b	1.8(2)	O(24)-H(24)...O(7) ^b	167(12)
N(8)-H(8)	1.00(2)	N(8)...O(16) ^c	3.12(1)	H(8)...O(16) ^c	2.17(1)	N(8)-H(8)...O(16) ^c	158(1)
N(23)-H(23)	1.00(1)	N(23)...N(18) ^d	2.84(1)	H(23)...N(18) ^d	1.87(1)	N(23)-H(23)...N(18) ^d	164(1)
Solvate 3							
O(2)-H(2)	1.00(4)	O(2)...O(24) ^a	2.651(5)	H(2)...O(24) ^a	1.70(4)	O(2)-H(2)...O(24) ^a	159(4)
N(8)-H(8)	1.00(1)	N(8)...O(1) ^f	2.992(6)	H(8)...O(1) ^f	2.00(1)	N(8)-H(8)...O(1) ^f	171(1)
N(23)-H(23)	1.00(5)	N(23)...N(18) ^g	2.862(5)	H(23)...N(18) ^g	1.87(1)	N(23)-H(23)...N(18) ^g	173(1)

^a 3 - x, 1 - y, 1 - z. ^b 2 - x, 1 - y, 1 - z. ^c 1 + x, y, z. ^d 1 - x, 1 - y, 2 - z. ^e 2 - x, -y, 2 - z. ^f 2 - x, -y, 1 - z. ^g 1 - x, 1 - y, -z.

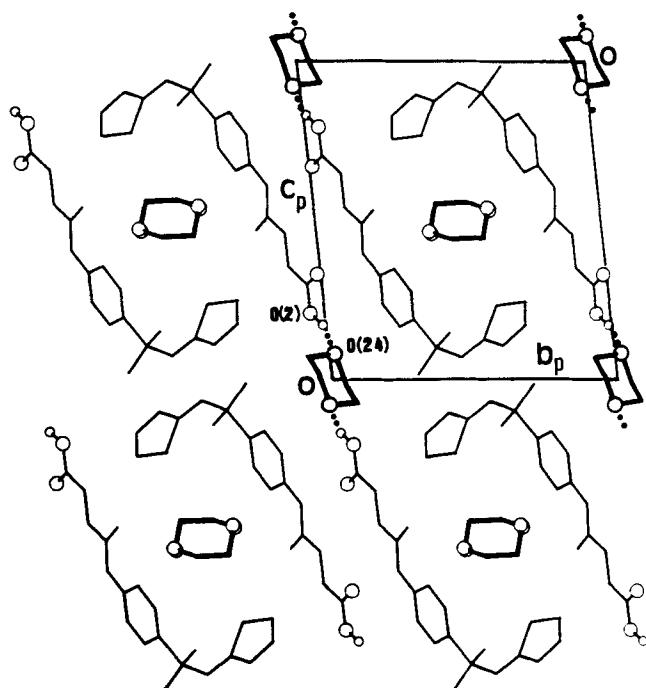


Figure 7—[100] projection of the structure of 3. Hydrogen bonds are indicated by dotted lines.

bonded to the host while the other half (at symmetry centers 0, 1/2, 1/2) are not. Both O atoms of the molecules of the former set accept a hydrogen bond, O(24)...H(2)-O(2) (Table 4), from the carboxylic group of SST. The structural results for these solvates are consistent with the results of thermal analysis which showed one-step desolvation for 1 and 2 and two-step desolvation for 3. In the latter case, it can be concluded that the first desolvation step involves the 1,4-dioxane molecules which do not engage in hydrogen bonding and which are therefore relatively loosely held in the crystal. Prior to anisotropic refinement, the atoms of these molecules had refined U_{iso} values twice as large, on average, as those of the hydrogen-bonded solvent molecules.

In view of the close similarity between the crystal structures of solvates 1 and 2, it was considered meaningful to compare the activation energies for their desolvation. These data were obtained using a published procedure¹⁸ and involved TG at various heating rates (β) and plotting $-\log \beta$ versus T^{-1} at several values of C , the fractional extent of desolvation. From the slopes of the resulting linear, parallel plots (a representative example is shown in Figure 8), the activation energies E_a for desolvation

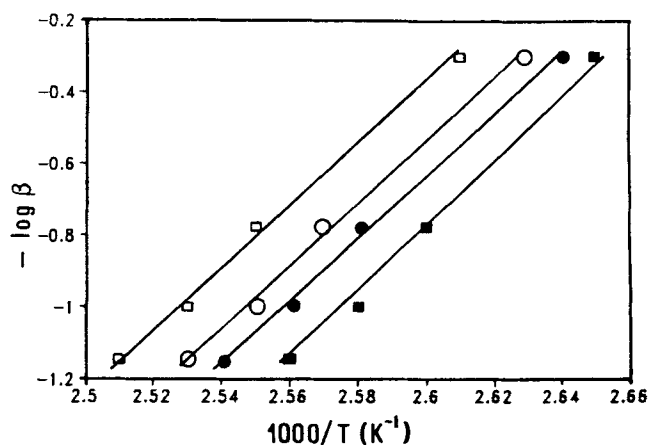


Figure 8—Plots of $-\log \beta$ vs T^{-1} for the desolvation of 1 for $C = 0.04$ (■), 0.08 (●), 0.12 (○), and 0.16 (□).

were estimated as 155 and 149 kJ mol⁻¹ for the 1-butanol and 1-pentanol solvates, respectively. Since the latter are nearly isostructural, it is not surprising that the E_a values are comparable. It is of interest to note, however, that these values are significantly larger than the estimates of E_a we obtained for the desolvation of the nearly isostructural 1,4-dioxane, chloroform, and tetrahydrofuran solvates of another sulfonamide drug, 5-methoxysulfadiazine (E_a range 94–103 kJ mol⁻¹) in which the solvent molecules are similarly trapped in cavities formed by the host lattice.³ The difference may be explained by the fact that, in 1 and 2, there is strong hydrogen bonding between host and guest, whereas there are no significant host-guest interactions of this type in the solvates of 5-methoxysulfadiazine. The E_a values obtained therefore reflect the distinction, based on crystallographic results, between “coordination clathrates” and “true clathrates”.

References and Notes

- Williams, R. A. D.; Kruk, Z. L. In *The Biochemistry and Pharmacology of Antibacterial Agents*; Croom Helm, Biology in Medicine Series: London, 1981; p28.
- Burger, A.; Grieser, U. *J. Sci. Pharm.* **1989**, *57*, 293–305.
- Caira, M. R.; Mohamed, R. *Supramolec. Chem.* **1993**, *2*, 201–207.
- Shirovani, K.; Suzuki, E.; Sekiguchi, K. *Chem. Pharm. Bull.* **1983**, *31*(6), 2085–2093.
- Shefter, E.; Higuchi, T. *J. Pharm. Sci.* **1963**, *52*, 781–791.
- Ballard, B. E.; Biles, J. A. *Steroids* **1963**, *4*, 273–278.
- Rodier, N.; Chauvet, A.; Masse, J. *Acta Crystallogr.* **1978**, *B34*, 218–221.

8. Yvon, K.; Jeitschko, W.; Parthé, E. *J. Appl. Crystallogr.* **1977**, *10*, 73-74.
9. Frenz, B. A., and Associates Inc. 1982, Structure Determination Package (College Station, TX).
10. Butt, G. L.; Deady, L. W.; Mackay, M. F. *J. Heterocycl. Chem.* **1988**, *25*, 321-326.
11. Sheldrick, G. M. SHELX-76 Program for Crystal Structure Determination; University of Cambridge: Cambridge, U.K. 1976.
12. *International Tables for X-ray Crystallography*; Kynoch: Birmingham, U.K. (present distributor: Kluwer Academic Publishers, Dordrecht, FRG) 1974; Vol. IV, pp 71-98.
13. Nardelli, M. *Comput. Chem.* **1983**, *7*, 95-98.
14. Motherwell, W. D. S. PLUTO, A Program for Plotting Molecular and Crystal Structures; University of Cambridge: Cambridge U.K., 1978.
15. Bar, I.; Bernstein, J. *J. Pharm. Sci.* **1985**, *74*, 255-263.
16. Caira, M. R.; Nassimbeni, L. R.; Niven, M. L.; Schubert, W-D.; Weber, E.; Dörpinghaus, N. *J. Chem. Soc. Perkin Trans 2* **1990**, 2129-2133.
17. Weber, E.; *Top. Curr. Chem.* **1987**, *140*, 1-20.
18. Flynn, J. H.; Wall, L. A. *J. Polym. Sci. Part B* **1966**, *4*, 323-328.

Acknowledgments

This work was supported the Foundation for Research Development (Pretoria) and the University of Cape Town.